Improved VBIC Model for SiGe HBTs With an Unified Model of Heterojunction Barrier Effects

Kyungho Lee, *Student Member, IEEE,* Dae-Hyung Cho, Kang-Wook Park, and Bumman Kim, *Senior Member, IEEE*

***Abstract*—An improved bipolar transistor model considering heterojunction barrier effect (HBE) in SiGe double heterojunction bipolar transistors is developed. The effect of barrier formation due to high level injection, which is related to the rapid degradations of the dc current gain (β) and cutoff frequency (f_T), is carefully investigated and analyzed. As the collector current becomes high, the conduction band barrier is induced and increased. It causes the saturation of collector current (J_C) due to the blocking of carrier transport, the sharp increase of base transit time (τ_B) due to the additional charge storage, the increase of base current (J_B) due to the increased recombination, and the decrease of intrinsic base resistance (R_{bi}) due to the increased charge and base pushout. Those phenomena are included into a vertical bipolar intercompany model (VBIC) compact model by employing a unified model of the HBE on J_C, J_B, τ_B, and R_{bi}. Furthermore, portions of τ_B and R_{bi} from the Kirk effect itself are modeled according to the high current model description and the new formulation of widened base, respectively. A full extraction of parameters has been performed and the modified VBIC model is applied. The modeling accuracy is significantly improved at the high current region for the dc and RF characteristics.**

***Index Terms*—Double heterojunction bipolar transistors (DHBTs), heterojunction barrier effect (HBE), high current effect, intrinsic base resistance, SiGe HBTs, transit time, vertical bipolar intercompany model (VBIC) model.**

I. Introduction

SiGe is the first practical bandgap-engineered silicon device. Due to the high-speed performance and mature silicon process, SiGe heterojunction bipolar transistors (HBT) has emerged as the technology of the choice for RFICs [1]. An accurate physically oriented model of the device is very important for designing a circuit, evaluating the process technology, and optimizing the device structure. Therefore, compact models are continuously updated and modified [2]. Because SiGe HBTs are typically modeled using conventional Si bipolar junction transistor (BJT)-based compact models such as vertical bipolar intercompany model (VBIC), Mextram, and high current model (HICUM), it is important to assess the accuracy of the models for capturing unique phenomena associated with the SiGe base layer. One such SiGe phenomenon is the heterojunction barrier effect (HBE), which is unavoidable in HBTs [3], [4].

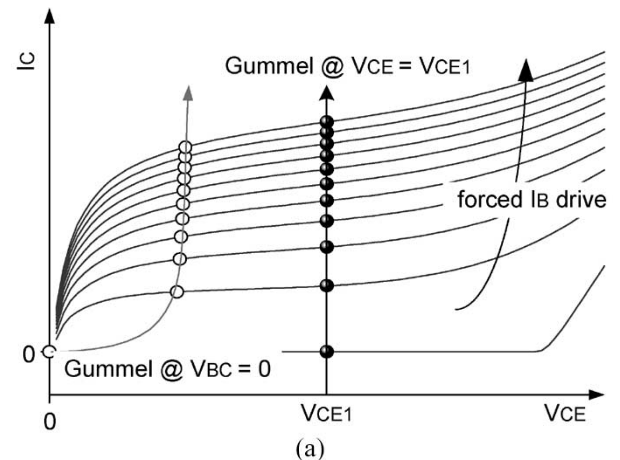

(a)

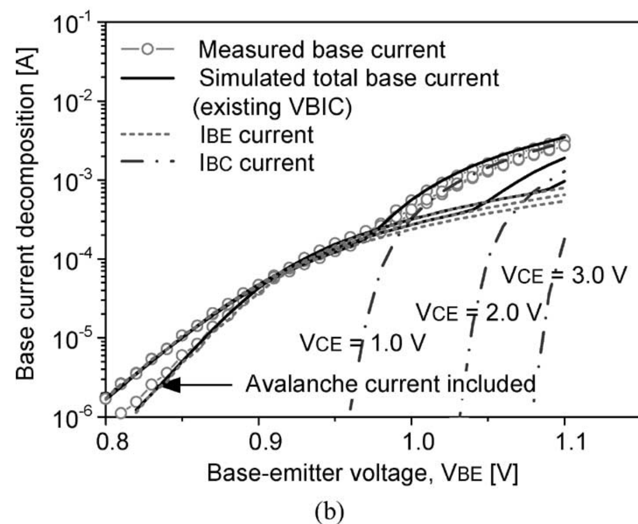

(b)

Fig. 1. (a) Typical dc *I–V* characteristics under the forced base current. (b) Measured base current and simulated base current using the VBIC model.

For the typical dc current–voltage *(I–V)* characteristics at the forced I_B condition, shown in Fig. 1(a), the decrease of current gain at the high V_{CE} region, where quasi-saturation is not significant, can be modeled as the saturation of J_C and/or the increase of J_B. Most of the compact models treat it as a J_C effect, such as the Webster–Rittner effect [high level injection (HLI)] [5], [6] and the Kirk effect [7]. However, the dominant β fall-off effect of SiGe HBTs arises from the sharp increase of J_B due to the HBE, although the J_C saturation due to the

Manuscript received October 20, 2005; revised January 13, 2006. This work was supported in part by the BK21 project of the Ministry of Education and Samsung Electronics Co., Ltd., Republic of Korea. The review of this paper was arranged by Editor J. Burghatz.

K. Lee and B. Kim are with the Department of Electrical Engineering, Pohang University of Science and Technology, Pohang 790-784, Korea (e-mail: bestee@postech.ac.kr).

D.-H. Cho is with the Core Development, Device Technology, System LSI Division, Samsung Electronics Co., Ltd., Yongin 449-711, Korea.

K.-W. Park is with the RF Development, Tech. Biz., System LSI Division, Samsung Electronics Co., Ltd., Yongin 449-711, Korea.

Digital Object Identifier 10.1109/TED.2006.871194

0018-9383/$20.00 © 2006 IEEE

HBE, Kirk effect, and HLI contributes partially. Fig. 1(b) shows the base currents, which include the measured base current, the simulated total base current with existing VBIC model, and decomposed components of the base-to-emitter current and base-to-collector current at the V_{CE} of 1.0, 2.0, and 3.0 V. At a low V_{CE}, the simulated total base current agrees well with measured data [collector–base (CB) junction turns on at a high V_{BE} because of R_C debiasing]. However, the results are quite different at higher V_{CE}s, where the HBE is important but mistakenly treated as the collector series resistance, since the CB heterojunction looks like an R_C/quasi-saturation in the Gummel plot at a low collector bias.

Several studies have been reported to investigate the formation of the conduction band barrier using their analytical models and to describe its dependence on J_C [8]–[12]. Their results are valuable references; however, their analytical derivations of J_C are mostly overestimated due to analytical studies without experimental verifications. Thus, they could not show clearly the saturation tendency. Joseph *et al.* [3] employ a numerical simulator to describe the operation of SiGe HBTs at the high current region. Liang *et al.* [4] propose an improved transit time model including the HBE in SiGe HBTs based on HICUM, and Fregonese *et al.* [13] derive a model for the base current increase using the result in [4]. Since they use the simpler model of the pushout base (W_{CIB}) and the constant barrier height, their approaches could not be accurate although the physical interpretations are very good.

In this paper, we have modeled the HBE on the saturation of the J_C, the sharp increase of J_B, and the drastic increase of τ_F, and the drop of R_{bi} in a unified manner. In our knowledge, this paper is the first one that treats all possible influences of HBEs. At first, we have carefully reviewed and derived the formation of current-induced conduction band barrier (ϕ_C) in our own way. From the calculated ϕ_C, the influences of HBE on J_C, J_B, τ_F, and R_{bi} are derived. Different from the previous J_C relations, a modified base charge (q_b) model with the two fitting parameters is introduced. R_{bi} is modeled considering both the Kirk effect and the HBE. The increase of transit time is also modified by partitioning components from the Kirk effect and HBE. The term of the Kirk effect is described following the HICUM; however, some of the parameters are redefined and modified. Lastly, by integrating the increase of transit time, the sharp increase of J_B is modeled.

To verify the validity of our model, modified formulations are implemented into the VBIC model in a unified manner, and the modified model is applied to a $5 \times 0.6 \times 5\ \mu\mathrm{m}^2$ SiGe HBT fabricated by 0.35-μm SiGe BiCMOS process technology at Samsung Electronics Co., Ltd. Modeling accuracy is significantly improved at a high current region for the dc and RF characteristics.

II. Review of Basic Physics and Analytical Derivation of HBEs

Different from a homojunction BJT, the HLI is negligible in HBTs due to its relatively high base doping level. Therefore, in typical single HBTs (SHBTs), the main reason that causes β and f_T falloffs at a high injection is the Kirk effect. The physical basis of Kirk effect is that the injected minority carrier concentration in the CB space charge region (SCR) is increased sufficiently to compensate the ionized donor density of the collector, causing the original CB electric field to collapsed and be pushed further into the collector region as the current density rises. The displacement of the CB electric field effectively increases the neutral base width (base pushout), leading to a falloff in the collector current gain and an increase in the base transit time [3], [7]. However, for double HBTs (DHBTs) such as SiGe HBTs, after the onset of the Kirk effect, the valence band offset (ΔE_V) at the vicinity of the CB heterojunction acts as a barrier for holes. Thus, the holes are accumulated at the CB junction when the electric field reaches zero at the point, neutralizing the mobile electron charge in the collector. This behavior leads to the formation of a positive electric field near the CB heterojunction, creating a electron barrier ϕ_C, which increases the minority carrier charge storage in the base with a corresponding increase in hole density to maintain charge neutrality.

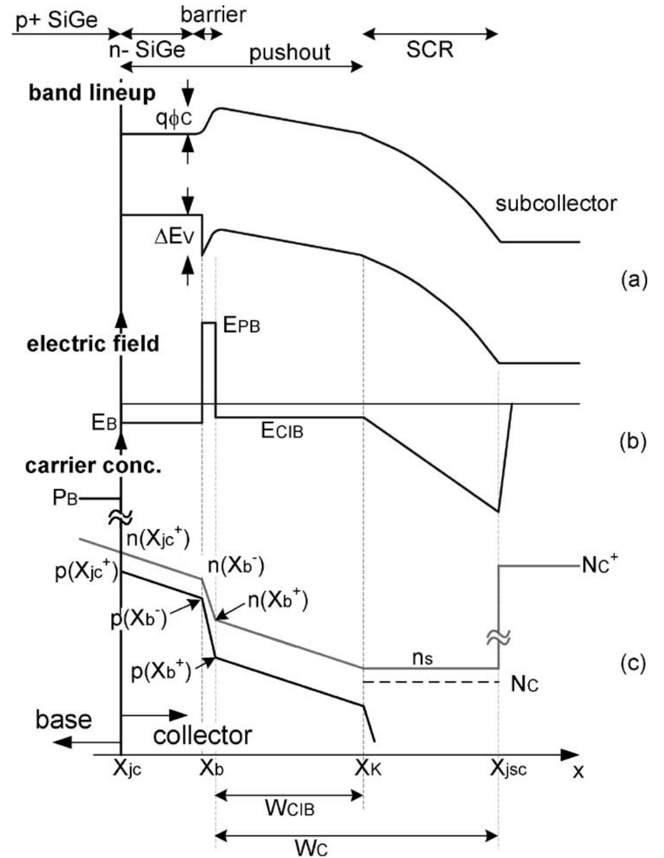

Fig. 2. (a) Energy band diagram. (b) Electric field profile. (c) Carrier concentration profiles in the SiGe HBT collector after base pushout. Drawings are rough and are not to scale.

A. Analytical Derivation of HBEs

Fig. 2 shows the energy band diagram, the electric field profile, and the carrier concentration profiles in the vicinity of the CB junction during formation of the barrier. Each profile agrees qualitatively with the results of the numerical simulations as

shown by Joseph *et al.* [3]. In the high injection operation, the collector layer is assumed to be depleted mostly with the peak electric field pushed to the subcollector interface. In the SiGe collector (n-SiGe), a small built-in field E_B that can arise from the compositional Ge grading is assumed. During barrier formation, there is a current-induced barrier field $E_{\rm PB}$, which is positive and is thereby inhibiting electron injection into the collector. Due to the onset of the current-induced base (CIB), there is also a small electric field $E_{\rm CIB}$, which is negative and a constant due to the fact that there is charge neutrality [8], [14]. The hole barrier is effectively reduced by ϕ_C as J_C increases. When the net hole barrier is reduced sufficiently, holes are spilled over into the collector to form a quasi-neutral region known as CIB.

The electron current may be found by estimating the electric field from the condition of identical hole drift and diffusion currents under the assumption of linear electron and hole distributions across the CIB region $W_{\rm CIB}$ [12], [14], i.e.,

$$J_C \simeq 2qD_{\rm nC}\frac{n\left(X_b^+\right)-n_S}{W_{\rm CIB}} \tag{1}$$

where q is the electronic charge, $D_{\rm nC}$ is the electron diffusivity of the collector, and n_S is the electron concentration in the collector high-field region, i.e., $n_S = J_C/qv_S$ (v_S is the saturation velocity). Thus, $n(X_b^+)$ and $p(X_b^+)$ are given by

$$n\left(X_b^+\right) \simeq J_C\frac{W_{\rm CIB}}{2qD_{\rm nC}}+n_S \tag{2}$$

$$p\left(X_b^+\right) = n\left(X_b^+\right)-n_S = J_C\frac{W_{\rm CIB}}{2qD_{\rm nC}}. \tag{3}$$

Knowing $n(X_b^+)$ and $p(X_b^+)$, we can get the electron and hole concentrations at X_b^-

$$n\left(X_b^-\right) = n\left(X_b^+\right)e^{\frac{q\phi_C}{(kT)}} \tag{4}$$

$$p\left(X_b^-\right) = p\left(X_b^+\right)e^{\frac{(\Delta E_V-q\phi_C)}{(kT)}} \tag{5}$$

which can be found once the current-induced conduction band barrier height is known. From (4), as ϕ_C is induced, $n(X_b^-)$ increases rapidly as the current level rises. It means a dynamic buildup of electrons at the collector end of the heterointerface. The accumulated charge contributes to the recombination in the quasi-neutral base and a reduction in the current gain. It also produces a rise in the base transit time and reduces the cutoff frequency.

The solution of Poisson's equation in the region of SCR (from X_K to $X_{\rm jc}$, where most of the $V_{\rm CB}$ drops across) of the collector gives

$$V_{\rm CB}+V_{\rm bi}+\phi_C = \frac{q}{2\epsilon_S}\left(n_S-N_C\right)\left(W_C-W_{\rm CIB}\right)^2 \tag{6}$$

where N_C and W_C are the doping concentration and the thickness of the collector, respectively, and ϵ_S is the permittivity of the collector. Thus, the thickness of the CIB region $W_{\rm CIB}$ is

$$W_{\rm CIB} = W_C-\sqrt{\frac{2\epsilon_S(V_{\rm CB}+V_{\rm biC}+\phi_C)}{q(n_S-N_C)}} \tag{7}$$

$$\simeq W_C\left(1-\sqrt{\frac{J_{\rm CK}-J_1}{J_C-J_1}}\right) \tag{8}$$

where $V_{\rm biC}$ is the built-in potential of the CB junction and $V_{\rm CB}$ is the applied CB voltage. $J_{\rm CK}$ (Kirk current density) and J_1 are defined as

$$J_{\rm CK} = qv_S\left[N_C+\frac{2\epsilon(V_{\rm CB}+V_{\rm biC})}{qW_C^2}\right] \tag{9}$$

$$J_1 = qv_SN_C. \tag{10}$$

Although $W_{\rm CIB}$ is a function of ϕ_C, $W_{\rm CIB}$ can be determined from (7) by neglecting ϕ_C, which is expected to be small compared to $V_{\rm CB}+V_{\rm bi}$ [8]. This expression of $W_{\rm CIB}$ is more accurate than that of the asymptotic equation of the HICUM model [4], [15].

Based on the references in [10] and [11], the induced conduction band barrier (ϕ_C), after the onset of base pushout, is given by

$$\phi_C = \frac{\Delta E_V}{q}+\frac{kT}{q}\ln\left\{\frac{1}{P_B}\left[n_S-N_C+\frac{J_CW_{\rm CIB}}{2qD_n}\right]\right\} \tag{11}$$

$$\simeq\frac{\Delta E_V}{q}+\frac{kT}{q}\times\ln\left\{\frac{1}{qv_SP_B}\left[J_C-J_1+\frac{v_SW_C}{2D_n}J_C\sqrt{\frac{J_{\rm CK}-J_1}{J_C-J_1}}\right]\right\} \tag{12}$$

where P_B is the doping concentration in the base.

In the above review and qualitative analysis of HBE, we have demonstrated the formation of ϕ_C and other secondary effects in the quantitative manner. The transistors used in this study have a planar self-aligned structure, deep- and shallow-trench isolation, a poly-Si emitter contact, and a graded epitaxial SiGe base. The detailed structure is shown in Fig. 3. The device has a SiGe base with 200 Å thick and doping of 5×10^{19} cm^{-3}, and a selectively implanted collector (SIC) with 7000 Å thick and doping of 1×10^{17} cm^{-3} for the high speed HBT (HS). In general, the graded base Ge profile begins and ends in the space-charge regions of the emitter–base (EB) and CB junctions, outside the neutral base. As shown in Fig. 3(b), the Si/SiGe heterointerface is placed at a location of 350 Å deeper into the collector and has 17.5% Ge content, which corresponds to ΔE_V of about 130 meV according to the rule of $0.74\times x_{\rm Ge}$. In order to reduce the impact of HBE, the SiGe layer should be placed deeper into the collector. However, it is limited by the amount of Ge that can be added because of the stability constraints of SiGe films [16]. The detailed device parameters used in this analysis are shown in Table. I.

The analytical results of $W_{\rm CIB}$ and ϕ_C are shown in Fig. 4. For comparison, the results of the low collector doping (N_C) of

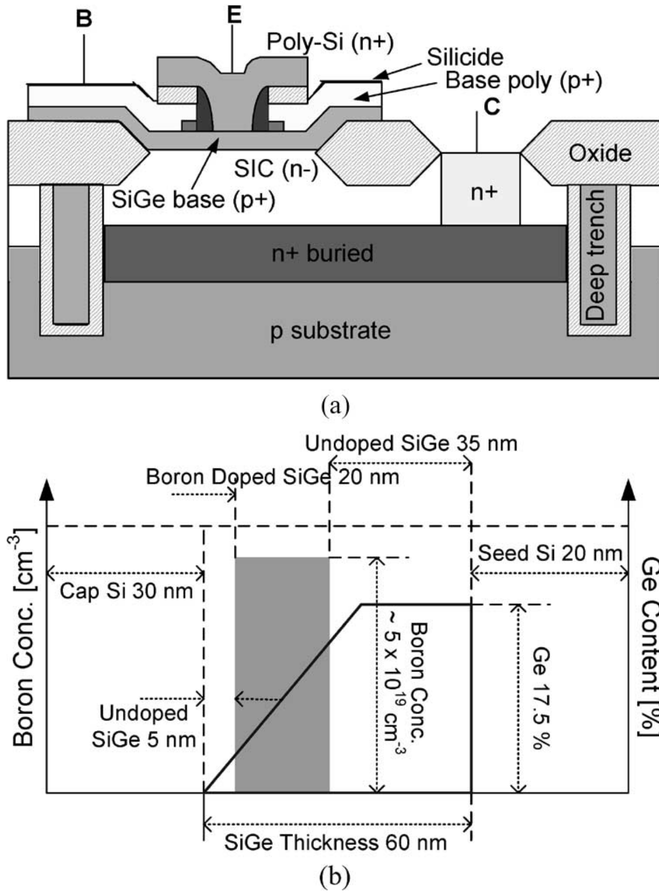

Fig. 3. (a) Schematic cross-section of a typical double poly-type SiGe HBT. (b) Schematic of epitaxial SiGe film used in an SiGe HBT. The film consists of a thin Si buffer layer, the compositionally graded SiGe layer, and an Si cap layer. The boron base doping is contained within the SiGe layer. Drawing is not to scale.

TABLE I
SiGe HBT DEVICE PARAMETERS USED IN THE ANALYSIS

Parameter	Value	Parameter	Value
A_E	$15\ \mu m^2$	m_n^*	$0.98m_0$
W_B	$200\mathring{A}$	n_i	$1.45\times10^{10}\ cm^{-3}$
W_C	$7000\mathring{A}$	v_S	$9.6\times10^{6}\ cm/s$
x_{bar}	$350\mathring{A}$	μ_{nC}	$765.5\ cm^2/V\cdot s$
P_B	$5\times10^{19}\ cm^{-3}$	μ_{nB}	$70.8\ cm^2/V\cdot s$
N_C	$1\times10^{17}\ cm^{-3}$	ΔE_V	$129.5\ meV$
N_{SC}	$2\times10^{19}\ cm^{-3}$	ΔE_C	$0\ meV$
ϵ_S	$1.05\times10^{-12}\ F/cm$	V_T	$0.0259\ V$

1×10^{16} cm^{-3} (for high voltage HBT, HV) are also added. An increase in $V_{\rm CE}$ enhances the electric field inside the junction and the $J_{\rm CK}$ of (9). Since high donor concentration requires high injected electrons to compensate the donor charge, $J_{\rm CK}$ increases as N_C increases. $W_{\rm CIB}$ increases sharply as N_C increases once base pushout starts. The rise in ϕ_C has similar behavior with $W_{\rm CIB}$, which initially increases rapidly after onset of base pushout and increases gradually toward saturation as shown in Fig. 4(b).

As mentioned earlier, the carrier concentration shown in Fig. 2(c) is determined from the current-induced barrier height. Fig. 5 shows the electron and hole concentrations as a function of J_C in the CB-SCR (n_S), before $[p(X_b^-)$ and $n(X_b^-)]$ and after $[p(X_b^+)$ and $n(X_b^+)]$ the barrier location.

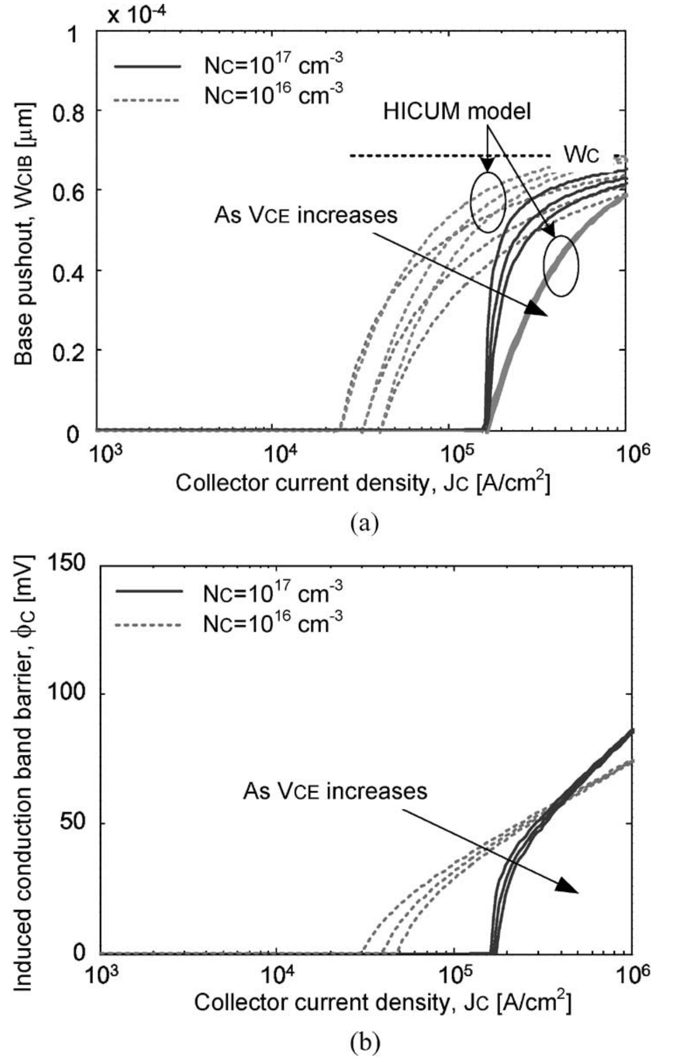

Fig. 4. Analytical results of the SiGe HBT biased at $V_{\rm CE} = 1.0$, 2.0, and 3.0 V for low voltage device, and 2.0, 4.0, and 6.0 V for high voltage device. (a) Thickness of base pushout $W_{\rm CIB}$. (b) Height of the induced conduction band barrier formation ϕ_C as a function of J_C. Results for $N_C = 10^{17}$ cm^{-3} (lined) and $N_C = 10^{16}$ cm^{-3} (dotted) are shown.

The electron concentration in the CB-SCR (n_S) rises slowly; however, the electron concentration at the end of the SiGe layer (base side) $n(X_b^-)$ rises sharply due to barrier formation with increasing J_C.

B. HBEs on the Collector Current and Base Resistance

Since the HLI effect in the base is negligible due to the high base doping level, the high current effect on typical SHBTs obeys the Kirk effect. However, in DHBTs such as SiGe HBTs, HBE influences J_C significantly, and this effect must be considered in the compact model. The widely used compact models such as Mextram and HICUM are based on the J_C saturation due to the Kirk effect, and they do not include the HBE on J_C. The VBIC compact model, which is familiar and is treated in this study, does not have the Kirk effect as well as the HBE on J_C. In this study, the Kirk effect and the HBE are lumped into one function, assuming both effects occur simultaneously and HBE influences more significantly on J_C. For the DHBT

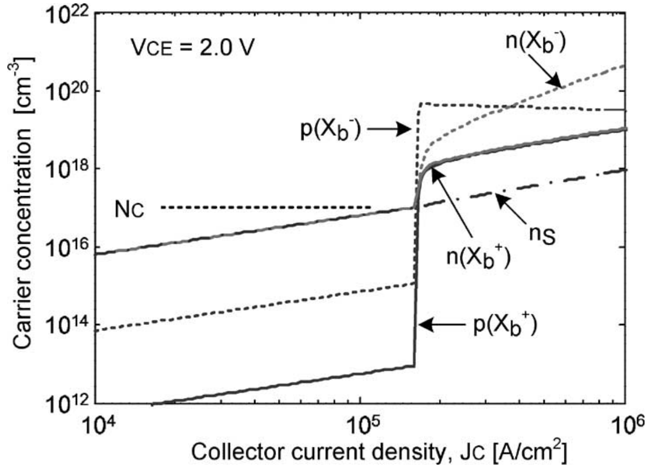

Fig. 5. Electron concentration of CB-SCR (n_S), hole and electron concentrations before [$p(X_b^-)$ and $n(X_b^-)$] and after [$p(X_b^+)$ and $n(X_b^+)$] the barrier location.

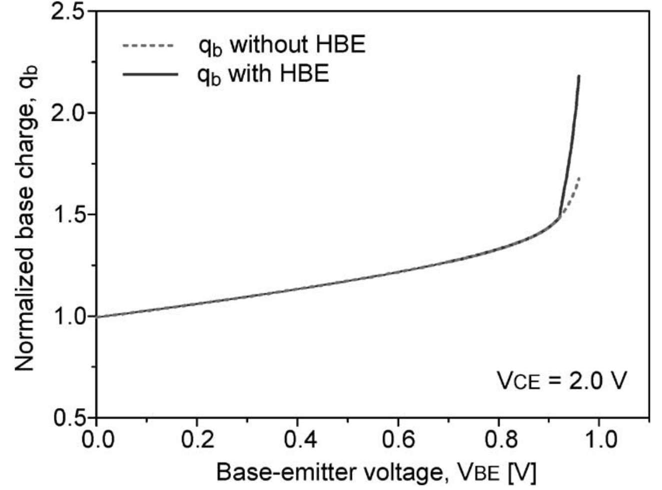

Fig. 6. Normalized base (hole) charge q_b without HBE (dotted) and with HBE (lined).

with a shallow heterointerface location (350 Å in this paper) due to the constraint of film stability [16], both effects occur simultaneously ($J_{\rm CK} = 1.692 \times 10^5$ A/cm^2 and $J_{\rm barrier} = 1.705 \times 10^5$ A/cm^2 at $V_{\rm CE} = 2.0$ V).

The HBE on J_C has been reported in [10], [12], and [17]. Since ϕ_C and $W_{\rm CIB}$ are a function of J_C, it is difficult to find an analytical form for the expression of J_C. Moreover, the reported results are somewhat overestimated. Therefore, a new empirical formulation of the HBE on J_C is proposed, introducing the two additional fitting parameters K_{ϕ_C} and n_{ϕ_C}, i.e.,

$$J_C = \frac{qD_n n_{i0}^2}{W_B P_B} e^{\frac{qv_{\rm BE}}{kT}} \frac{1 + K_{\phi_C}}{1 + K_{\phi_C} e^{\frac{q\phi_C}{\left(n_{\phi_C} kT\right)}}} \tag{13}$$

where $qD_n n_{i0}^2/W_B P_B$ is a collector saturation current, and the other HBE term represents the normalized base charge (q_b). Therefore, the q_b in the existing VBIC model [18] is modified by the HBE component and is given by

$$q_b = \frac{1}{2} \frac{\left(q_1 + \sqrt{q_1^2 + 4q_2^2}\right)}{q_3} \tag{14}$$

where q_1 and q_2 represent the Early effect and HLI effect, respectively. Thus, the additional HBE component q_3 is given by

$$q_3 = \frac{1 + K_{\phi_C}}{1 + K_{\phi_C} e^{\frac{q\phi_C}{\left(n_{\phi_C} kT\right)}}}. \tag{15}$$

Fig. 6 shows the q_b on the $V_{\rm BE}$ at a $V_{\rm CE}$ of 2 V, where we can find a sharp increase of q_b at a high injection operation.

Using the formulations, the HBE on the intrinsic base resistance ($R_{\rm bi}$) is investigated. Since $R_{\rm bi}$ is inversely proportional to the base conductivity and base width [19], both the HBE and the Kirk effect are considered to model the $R_{\rm bi}$ behavior. Basically, the intrinsic base resistance of the existing VBIC model with RBI$/q_b$, where RBI is a VBIC model parameter, and only the HLI and Early effects are included through q_b. We have included the HBE on $R_{\rm bi}$, replacing the existing q_b with the modified q_b in (14). An additional term describing the Kirk effect can be obtained by

$$R_{\rm bi,CIB} = K_{\rm rb} {\rm RBI} \frac{P_B}{p_{\rm CIB}} \frac{W_B}{W_{\rm CIB}} \frac{\mu_{\rm nB}}{\mu_{\rm CIB}(p_{\rm CIB})} \tag{16}$$

where $p_{\rm CIB}$ is the average hole concentration in the CIB region and $K_{\rm rb}$ is the fitting parameter. Here, $W_{\rm CIB}$, $p_{\rm CIB}$, and $\mu_{\rm CIB}$ are the dependent on J_C. Mobility is calculated with the popular Arora's mobility model [20]. Since the hole profile is assumed linear, the average hole concentration is found as

$$p_{\rm CIB} = \frac{p\left(X_b^+\right)}{2}. \tag{17}$$

Since each resistance of the two regions contributes in parallel, the modified intrinsic base resistance model can be expressed as

$$R_{\rm bi,mod} = \frac{\rm RBI}{q_b} \| R_{\rm bi,CIB}. \tag{18}$$

Fig. 7 shows the extracted and model simulated intrinsic base resistances on the J_C at a $V_{\rm CE}$ of 2.0 V. According to Lee *et al.* [21], $R_{\rm bi}$ is carefully extracted after the exact deembedding of extrinsic parasitic elements using S-parameter measurements. As shown, the modeling results are in good agreement with the extracted data. We also found that the intrinsic base resistance depends on both the HBE and the Kirk effect, and the widened base is the dominant factor of $R_{\rm bi}$ decrease.

C. HBEs on the Transit Time and Base Current

Usually, the high current effect on transit time is modeled as the Kirk effect of the increased effective base width [7] and the increased CB capacitance [14]. As shown in the intrinsic base resistance, both the Kirk effect and the HBE affect the increase of transit time. Liang *et al.* [4] have proposed an improved transit time model including the HBE in SiGe HBTs based on the HICUM model. Although their results are in good agreement with the extracted data, since they use the asymptotic expression of $W_{\rm CIB}$ and the constant barrier height, their

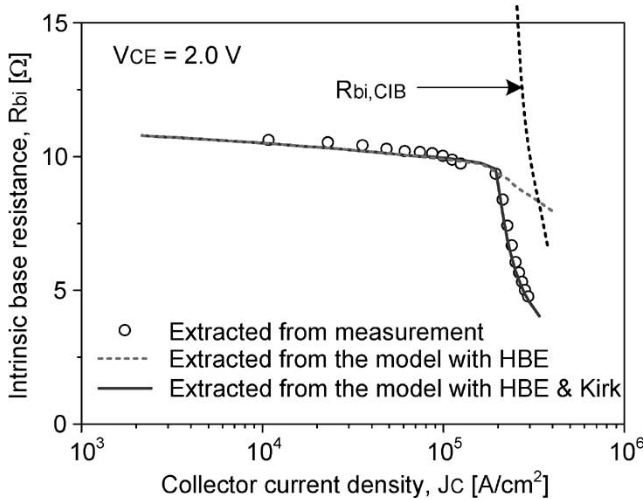

Fig. 7. Intrinsic base resistance as a function of collector–current density ($V_{\rm CE} = 2$ V).

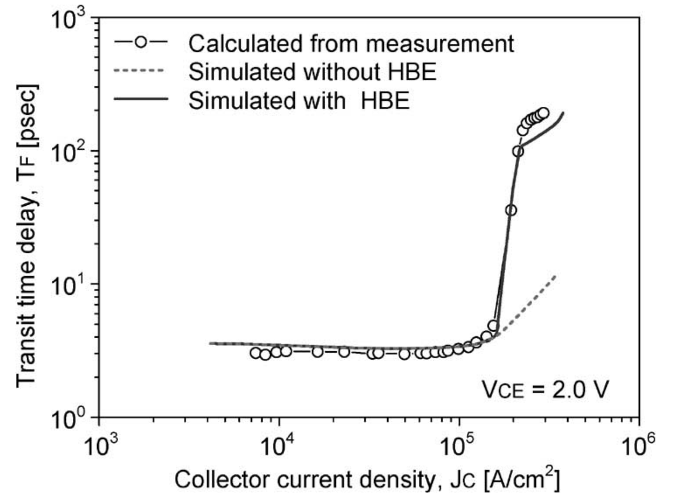

Fig. 8. Measurement-calculated ($- \circ -$) and model-calculated [without HBE (dotted) and with HBE (lined)] transit time delay T_F of the $5 \times 0.6 \times 5.0\ \mu{\rm m}^2$ SiGe HBT as a function of collector current densities at $V_{\rm CE} = 2.0$ V.

approach does not include the current dependency of the barrier height.

Transit frequency f_T is defined as the frequency at which the small-signal current gain becomes unity and is given by

$$\frac{1}{2\pi f_T} = \tau_F + \frac{C_{\rm JE} + C_{\rm BC}}{g_m} + (R_{\rm CX} + R_E)C_{\rm BC} \tag{19}$$

where τ_F is the total transit time, $C_{\rm JE}$ and $C_{\rm BC}$ are the EB junction depletion and CB capacitances, respectively, $R_{\rm CX}$ and R_E are the extrinsic collector and emitter resistances, respectively, and g_m is the transconductance defined as I_C/V_T.

Transit time (τ_F) itself can be partitioned into a low-current component τ_{F0} and a high-current component $\Delta\tau_F$ as

$$\tau_F = \tau_{F0} + \Delta\tau_F. \tag{20}$$

The high current term of transit time $(\Delta\tau_F)$ itself can also be partitioned into components from the Kirk effect and HBE, i.e.,

$$\Delta\tau_F = \Delta\tau_{B,\rm HBE} + \Delta\tau_{B,K} + (R_E + R_{\rm CX})\Delta C_{{\rm BC},K} \tag{21}$$

where $\Delta\tau_{B,\rm HBE}$ is from the charge accumulation due to HBE, $\Delta\tau_{B,K}$ is from the widened base due to Kirk effect [7], and the other term is from the increased $C_{\rm BC}$ due to Kirk effect [14]. In order to consider the latter two terms, the phenomena are modeled according to the HICUM description [15]. However, some of the parameters are redefined. The current density $J_{\rm CK}$ at which the base pushout starts is defined in (9). The normalized thickness of the base pushout is replaced (23). Thus, HICUM formulations are modified as

$$\Delta\tau_{B,K} = \tau_{\rm hCs} w^2 \left[1 + \frac{2J_{\rm CK}}{J_C\sqrt{w^2 + a_{\rm hc}}}\right] \tag{22}$$

$$w = \frac{W_{\rm CIB}}{W_C} \tag{23}$$

where $\tau_{\rm hCs}$ and $a_{\rm hc}$ are the fitting parameters. The emitter charge contribution term is adopted from the HICUM model as

$$\Delta\tau_{Ef0} = \tau_{Ef0}\left(\frac{J_C}{J_{\rm CK}}\right)^{g\tau E} \tag{24}$$

where τ_{Ef0} and $g\tau E$ are the fitting parameters.

From the relation in (4) and Liang's derivation [4], the additional HBE term $\Delta\tau_F$ can be derived by

$$\Delta\tau_{B,\rm HBE} = K_{\tau,b}\left(e^{\frac{q\phi_C}{(kT)}} - 1\right) \tag{25}$$

$$= K_{\tau,b}\left[e^{\frac{\Delta E_V}{(kT)}}\left\{\frac{1}{qv_SP_b}\left(J_C - J_1 + \frac{v_SW_C}{2D_{\rm nC}} \times J_C\sqrt{\frac{J_{\rm CK} - J_1}{J_C - J_1}}\right)\right\} - 1\right] \tag{26}$$

where $K_{\tau,b}$ is the fitting parameter. Fig. 8 shows the transit time delay (τ_F) as a function of J_C at a $V_{\rm CE}$ of 2.0 V. Extraction is performed in the conventional manner (the subtraction of g_m delay and neglect of the emitter charging delay at a low current region). Both the Kirk effect and the HBE influence the transit time at high injection operation. After the onset of the two effects, the transit time increases drastically. The comparison shows that the modified model captures accurately the transit time at the high injection operation.

Lastly, the HBE on the base current is analyzed. The sudden increase in J_B accompanying the onset of HBE in a SiGe HBT is explained by the accumulation of holes in the base region. Fregonese *et al.* [13] have derived a model for the base current increase using the modified transit time in [4]. However, for the same reason in [4], their physical analysis is not very accurate.

The charge stored in the base and collector related to the HBE can be calculated as follows. Since $\Delta\tau_{B,\rm HBE}$ is given by

TABLE II
HBE-RELATED PARAMETERS

Parameter	Value	Parameter	Value	Parameter	Value
K_{ϕ_C}	0.1	n_{ϕ_C}	2.0	K_{rb}	0.3
$K_{\tau,b}$	6.5 p	$\tau_{r,b}$	60 p	a_{HBE}	1e-10

$d\Delta Q_B/dJ_C$, ΔQ_B is obtained by integrating transit time with respect to J_C as

$$\Delta Q_{B,\mathrm{HBE}}(J_C) \equiv \int \Delta\tau_{B,\mathrm{HBE}} dJ_C \tag{27}$$

$$= K_{\tau,b} e^{\frac{\Delta E_V}{(kT)}} \times \left[\frac{1}{qv_S P_B} \left\{ \frac{1}{2} J_C^2 - J_1 J_C + \frac{v_S W_C}{3D_n} \left(\frac{J_{\mathrm{CK}} - J_1}{J_C - J_1} \right)^{\frac{1}{2}} \times (J_C - J_1)(J_C + 2J_1) \right\} \right] - K_{\tau,b} J_C. \tag{28}$$

Therefore, we deduce the expression of the stored charge as a function of J_C as

$$\Delta Q_{B,\mathrm{HBE}} = \Delta Q_b(J_C) - \Delta Q_b(J_{\mathrm{CK}}). \tag{29}$$

Using the continuity current equation and assuming Shockley–Read–Hall (SRH) recombination [13], [23], we obtain

$$\frac{d\Delta J_B}{dx} = qR = q\frac{\Delta p}{\tau_{r,b}} \tag{30}$$

where $\tau_{r,b}$ is a fitting parameter for the recombination time. By integrating (30) over the whole transistor, we obtain

$$\Delta J_B = \frac{\Delta Q_{B,\mathrm{HBE}}}{\tau_{r,b}}. \tag{31}$$

Table II shows the HBE-related fitting parameters used in this paper, where a_{HBE} is used in the smoothing function of W_{CIB} and ϕ_C.

Fig. 9 shows the internal Gummel plot and its corresponding current gain at a V_{CE} of 2.0 V. It is deembedded with the series resistance (R_E, R_{BX}, and R_{BI}) from the measurement data. The internal base–emitter voltage (V_{BEi}) is obtained with the Ning–Tang method [22], which neglects the bias-dependent effect of R_{bi} and avoids the region where I_{BC} is significant. As shown in the figures, HBE causes the saturation of J_C and the sharp increase of J_B. And the major factor of β falloff under the HBE is the increase of J_B. A newly developed model has a good agreement with the Gummel plot of the deembedded measurement.

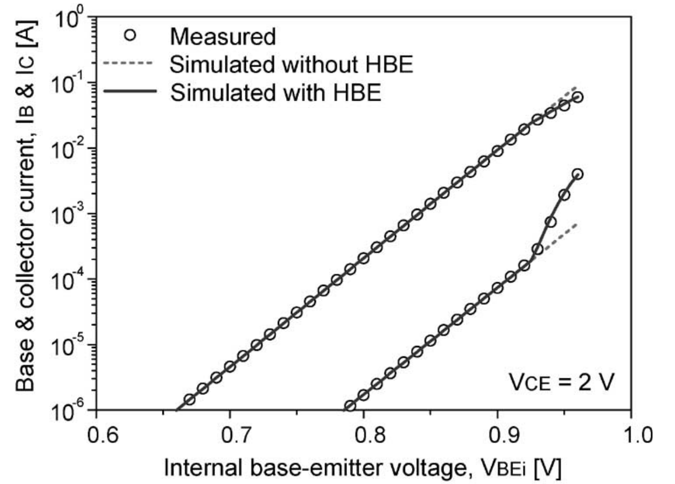

(a)

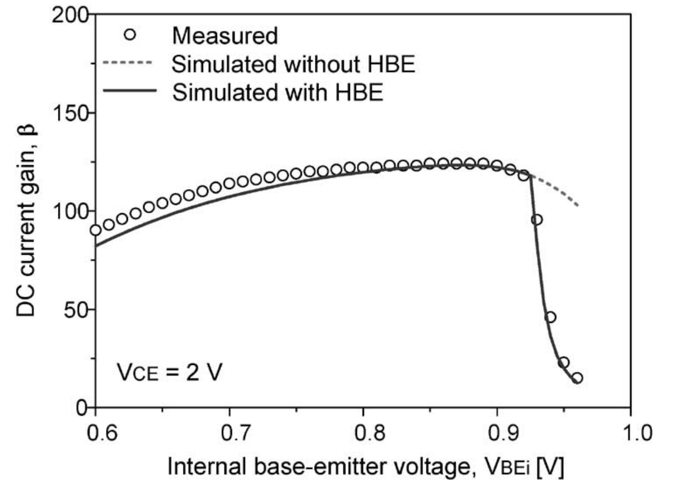

(b)

Fig. 9. Measurement deembedded (○) and simulated (lined) (a) internal Gummel plot, (b) corresponding current gain β of the $5 \times 0.6 \times 5.0\ \mu\mathrm{m}^2$ SiGe HBT as a function of intrinsic base-emitter voltage, at $V_{\mathrm{CE}} = 2.0$ V.

TABLE III
MAJOR PARAMETERS OF THE IMPROVED VBIC MODEL

Parameter	Value	Parameter	Value	Parameter	Value
NF	1.01	IS	10.16 a	NR	1.01
VEF	256.28	VER	3.18	IKF	0.40
NEI	1.03	IBEI	0.14 a	NEN	1.62
IBEN	0.16 f	NCI	1.20	IBCI	90.09 f
NCN	1.54	IBCN	0.23 p	AVC1	2.40
AVC2	15.08	RE	1.91	RBX	2.16
RBI	11.70	RCX	3.32	RCI	33.0
GAMM	2.78 p	VO	51.67	RTH	386
CJE	77.16 f	PE	0.84	ME	0.30
CJC	44.87 f	PC	0.60	MC	0.26
TF	3.04	VTF	1.5	ahc	0.002
τ_{hCs}	2.0 p	τ_{Ef0}	0.1 p	$g_{\tau E}$	2.0

III. MODEL IMPLEMENTATION INTO VBIC, EXPERIMENTAL VERIFICATION, AND DISCUSSION

In order to modify the existing VBIC compact model, the model is implemented to a symbolically defined device (SDD) in Agilent ADS. The four elements of the existing VBIC model are modified. They are I_{TZF}, I_{BE}, $Q_{\mathrm{BE}}(\tau_F)$, and RBI/q_b as mentioned in Section II. A smoothing function [4] is used for W_{CIB} and ϕ_C in order to eliminate discontinuity. For example

$$\phi_{\mathrm{CC}} = \frac{\phi_C + \sqrt{\phi_C^2 + a_{\mathrm{HBE}}}}{1 + \sqrt{1 + a_{\mathrm{HBE}}^2}} \tag{32}$$

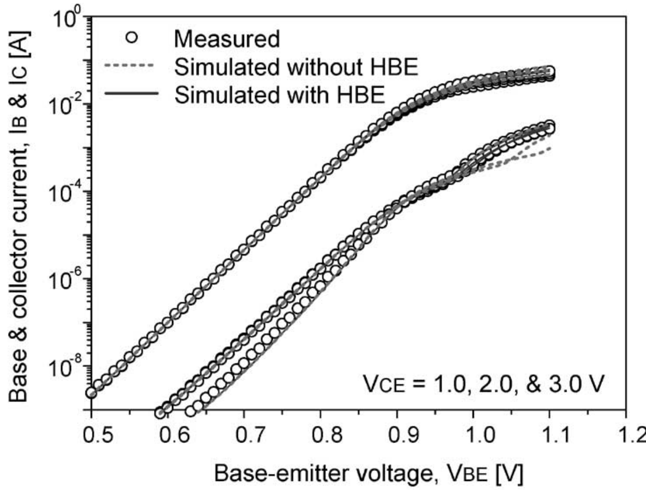

(a)

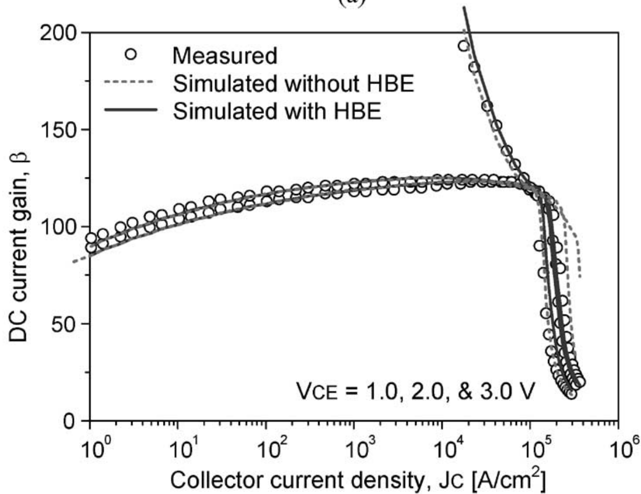

(b)

Fig. 10. Measured (○) and simulated [without HBE (dotted) and with HBE (lined)] (a) Gummel plot and (b) corresponding current gain β of the $5 \times 0.6 \times 5.0\ \mu\mathrm{m}^2$ SiGe HBT at $V_{\mathrm{CE}} = 1.0, 2.0,$ and 3.0 V.

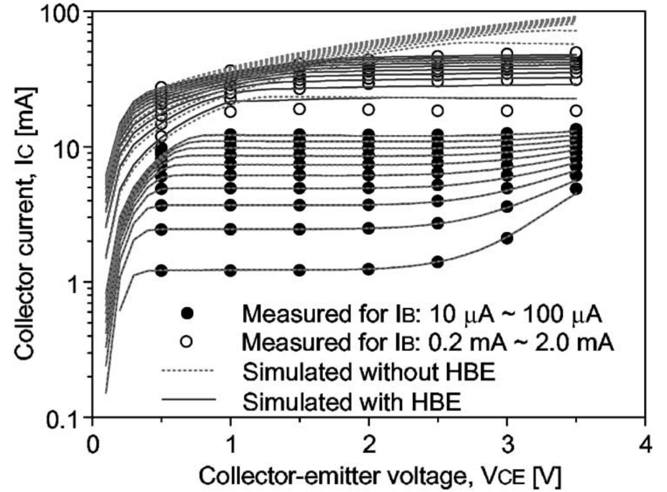

(a)

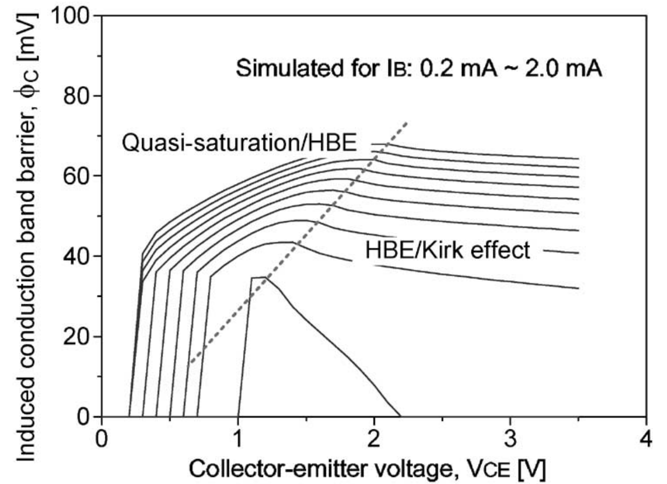

(b)

Fig. 11. (a) Measured (● for low injection and ○ for high injection) and simulated [without HBE (dotted) and with HBE (lined)] dc *I–V* characteristics of the $5 \times 0.6 \times 5.0\ \mu\mathrm{m}^2$ SiGe HBT under forced base currents of 10–100 μA and 0.2–2.0 mA. (b) Corresponding calculated results of the induced conduction band barrier height for a base current of 0.2–2.0 mA.

where a_{HBE} is the adjustment parameter. The collector current of the existing VBIC model is I_{TF} defined as $I_S \cdot e^{V_{\mathrm{BEi}}/(N_F V_T)}$, and I_{TZF} (or J_{TZF}) can be calculated with I_{TF}/q_b and emitter area. Then, the induced barrier (denoted $\phi_{C,B}$) is reformulated as a function of J_{TZF} once the real collector current density (J_{TZF}) is determined. After that, the transit time and the base current are determined from the calculation with $\phi_{C,B}$.

In order to validate the newly developed model, a complete extraction of the VBIC model parameters has been performed on the SiGe HBT of $5 \times 0.6 \times 5\ \mu\mathrm{m}^2$ from the SiGe BiCMOS technology of Samsung Electronics Company, Ltd. The major parameters of the improved VBIC model are listed in Table III. Fig. 10 shows the measured and model-simulated Gummel plot and its corresponding current gain of the SiGe HBT at $V_{\mathrm{CE}} = 1.0, 2.0,$ and 3.0 V, with and without the HBE. They have good agreements each other. For the same device, the measured and simulated dc *I–V* characteristics under a forced base current are compared. As shown in Fig. 11(a), in the low current region with base current of 10–100 μA, where the high current effect is not significant, the simulated results are well fitted with measured data, without the HBE. However, in the high current region of 0.2–2.0 mA, where several high current effects occur, the measured and simulated results without the HBE have large discrepancies except at the low collector bias. The accuracy of the simulated result with the HBE is improved significantly. Fig. 11(b) shows the calculated results of the induced conduction barrier height for a base current of 0.2–2.0 mA. Barrier formation starts roughly at a base current between 0.2 and 0.4 mA. At low collector biases, despite the induced conduction band barrier, the quasi-saturation effect dominates the dc *I–V* characteristics.

Fig. 12 compares the cutoff frequencies as a function of J_C using the transit time model implemented, showing significantly improved accuracy in the wide bias range. The high speed (HS) and the high voltage (HV) SiGe HBTs are also compared as shown in Fig. 13. The collector biases are selected 2.0 and 4.0 V for HS and HV devices, respectively, which

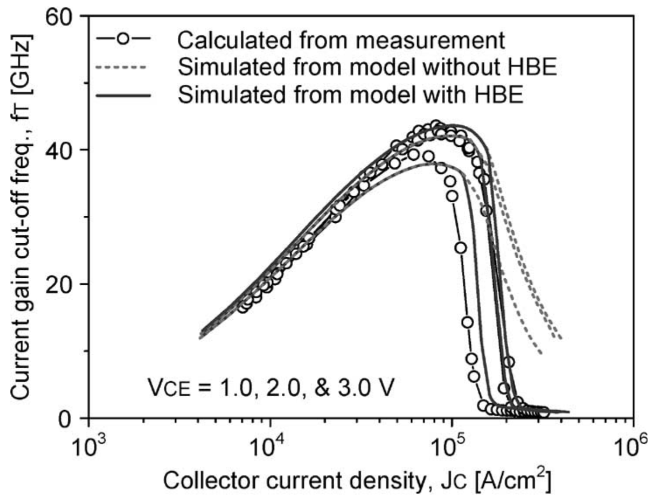

Fig. 12. Measurement-calculated $(-\circ-)$ and model-simulated [without HBE (dotted) and with HBE (lined)] current gain cutoff frequencies f_T of the $5 \times 0.6 \times 5.0\ \mu\text{m}^2$ SiGe HBT as a function of collector current densities at $V_{\text{CE}} = 1.0, 2.0,$ and 3.0 V.

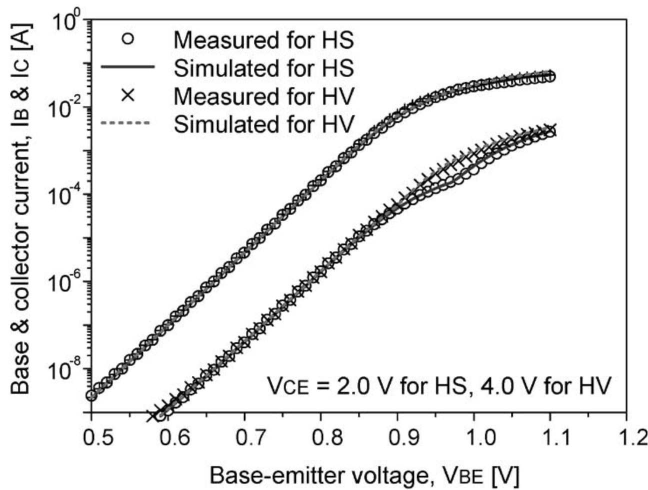

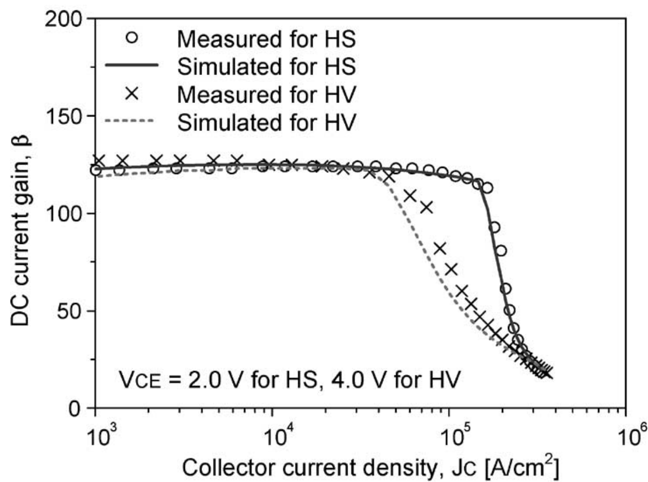

Fig. 13. Measured (○ for HS and × for HV) and simulated (lined for HS and dotted for HV) (a) Gummel plot and (b) corresponding current gain of the $5 \times 0.6 \times 5.0\ \mu\text{m}^2$ SiGe HBTs at $V_{\text{CE}} = 2.0$ V for HS and 4.0 V for HV.

avoid significant quasi-saturation. They also fit very well and follow the tendencies of ϕ_C and W_{CIB} (Fig. 4). These results validate the usefulness of the improved VBIC model including the unified model of HBE.

IV. Conclusion

In this paper, the unified model of high injection HBE is developed. A comprehensive investigation of the physics of the HBE and its impact on the behavior of SiGe HBTs has been performed. As the collector current becomes high, the conduction band barrier is induced and increased. It gives rise to the saturation of collector current due to the blocking of carrier transport by the barrier, the increased transit time due to charge storage, the increase of base current due to increased recombination, and the drop of intrinsic base resistance due to increased base charge and base pushout. From the accurate derivation of ϕ_C and W_{CIB}, the modified models of J_C, J_B, τ_F, and R_{bi} have been added inside VBIC, which has been implemented using the SDD in Agilent ADS. A full parameter of the modified VBIC model has been extracted for the simulation. The simulation results show the significantly improved accuracy of our model at the high current region for the dc and RF characteristics.

References

[1] D. L. Harame, D. C. Ahlgren, D. D. Coolbaugh, J. S. Dunn, G. G. Freeman, J. D. Gillis, R. A. Groves, G. N. Hendersen, R. A. Johnson, A. J. Joseph, S. Subbanna, A. M. Victor, K. M. Watson, C. S. Webster, and P. J. Zampardi, "Current status and future trends of SiGe BiCMOS technology," *IEEE Trans. Electron Devices*, vol. 48, no. 11, pp. 2575–2594, Nov. 2001.

[2] Compact Model Council of EIA in USA. [Online]. Available: http// www.eigroup.org/cmc

[3] A. J. Joseph, J. D. Cressler, D. M. Richey, and G. Niu, "Optimization of SiGe HBT's for operation at high current densities," *IEEE Trans. Electron Devices*, vol. 46, no. 7, pp. 1347–1354, Jul. 1999.

[4] Q. Liang, J. D. Cressler, G. Niu, R. M. Malladi, K. Newton, and D. L. Harame, "A physics-based high-injection transit-time model applied to barrier effects in SiGe HBTs," *IEEE Trans. Electron Devices*, vol. 49, no. 10, pp. 1807–1813, Oct. 2002.

[5] W. M. Webster, "On the variation of junction-transistor current amplification factor with emitter current," *Proc. IRE*, vol. 42, no. 6, pp. 914–916, Jun. 1954.

[6] E. S. Rittner, "Extension of the theory of the junction transistor," *Phys. Rev.*, vol. 94, no. 5, pp. 1161–1171, Jun. 1954.

[7] C. T. Kirk, "A theory of transistor cutoff frequency falloff at high current densities," *IRE Trans. Electron Devices*, vol. 9, no. 3, pp. 164–174, Mar. 1962.

[8] K. P. Roenker, S. A. Alterovitz, and C. H. Mueller, "Device physics analysis of parasitic conduction band barrier formation in SiGe HBTs," in *Proc. Silicon Monolithic Integrated Circuits RF Systems Dig.*, 2000, pp. 182–186.

[9] M. Yee and P. A. Houston, "High current effects in double heterojunction bipolar transistors," *Semicond. Sci. Technol.*, vol. 20, no. 5, pp. 412–417, May 2005.

[10] J. S. Yuan and J. Song, "Base–collector heterojunction barrier effect of the SiGe HBT at high current densities," in *IEDM Tech. Dig.*, 1998, pp. 101–104.

[11] B. Mazhari and H. Morkoc, "Effect of collector–base valence band discontinuity on Kirk effect in double heterojunction bipolar transistors," *Appl. Phys. Lett.*, vol. 59, no. 17, pp. 2162–2164, Oct. 1991.

[12] P. E. Cottrell and Z. Yu, "Velocity saturation in the collector of $\text{Si/Ge}_x\text{Si}_{1-x}\text{/Si}$ HBT's," *IEEE Electron Device Lett.*, vol. 11, no. 10, pp. 431–433, Oct. 1990.

[13] S. Fregonese, T. Zimmer, C. Maneux, and P. Y. Sulima, "Barrier effects in SiGe HBT: Modeling of high-injection base current increase," in *Proc. IEEE BCTM*, 2004, pp. 104–107.

[14] W. Liu and J. S. Harris, "Current dependence of base–collector capacitance of bipolar transistors," *Solid State Electron.*, vol. 35, no. 8, pp. 1051–1057, Aug. 1992.
[15] M. Schröter and T.-Y. Lee, "Physics-based minority charge and transit time modeling for bipolar transistors," *IEEE Trans. Electron Devices*, vol. 46, no. 2, pp. 288–300, Feb. 1999.
[16] D. L. Harame, J. H. Comfort, J. D. Cressler, E. F. Crabbé, J. Y.-C. Sun, B. S. Meyerson, and T. Tice, "Si/SiGe epitaxial-base transistors—Part I: Materials, physics, and circuits," *IEEE Trans. Electron Devices*, vol. 42, no. 3, pp. 455–468, Mar. 1995.
[17] J. W. Slotboom, G. Streutker, A. Pruijmboom, and D. J. Gravesteijin, "Parasitic energy barriers in SiGe HBT's," *IEEE Electron Device Lett.*, vol. 12, no. 9, pp. 486–488, Sep. 1991.
[18] C. C. McAndrew, J.A. Seitchik, D. F. Bowers, M. Dunn, M. Foisy, I. Getreu, M. McSwain, S. Moinian, J. Parker, D. J. Roulston, M. Schröter, P. V. Wijnen, and L. F. Wagner, "VBIC95, the vertical bipolar inter-company model," *IEEE J. Solid-State Circuits*, vol. 31, no. 10, pp. 1476–1483, Oct. 1996.
[19] F. Hébert and D. J. Roulston, "Voltage- and current-dependent model for the base resistance of bipolar transistors," *IEEE Trans. Electron Devices*, vol. 35, no. 10, pp. 1696–1699, Oct. 1988.
[20] N. D. Arora, J. R. Hauser, and D. J. Roulston, "Electron and hole mobilities in silicon as a function of concentration and temperature," *IEEE Trans. Electron Devices*, vol. ED-29, no. 2, pp. 292–295, Feb. 1982.
[21] K. Lee, K. Choi, S.-H. Kook, D.-Y. Cho, K.-W. Park, and B. Kim, "Direct parameter extraction of SiGe HBTs for the VBIC bipolar compact model," *IEEE Trans. Electron Devices*, vol. 52, no. 3, pp. 375–384, Mar. 2005.
[22] T. H. Ning and D. D. Tang, "Method for determining the emitter and base series resistances of bipolar transistors," *IEEE Trans. Electron Devices*, vol. ED-31, no. 4, pp. 409–412, Apr. 1984.
[23] S. M. Sze, *Physics of Semiconductor Devices*, 2nd ed. New York: Wiley, 1981.
[24] I. E. Getreu, *Modeling the Bipolar Transistor*. New York: Elsevier, 1978.

Kyungho Lee (S'04) was born in Miryang, Korea, on 1975. He received the B.S. degree in electronics and electrical engineering from Kyungpook National University, Daegu, Korea, in 1999, the M.S. degree in electronics and electrical engineering from Pohang University of Science and Technology, Pohang, Korea, in 2001, and is currently working toward the Ph.D. degree in electronics and electrical engineering.

His research interests include device design and fabrication of high-speed InP-based HBTs and RF modeling of SiGe HBTs and MOSFETs.

Dae-Hyung Cho received the Ph.D. degree in electrical engineering from the University of Illinois at Urbana-Champaign in 1995.

From 1983 to 1990, he was with Samsung Electronics Company, Korea, where he worked on device modeling and circuit simulation. Until 1995, he was a Research Assistant at the Beckman Institute for Advanced Science and Technology, Urbana, IL. In 1995, he joined the System IC Division, Hyundai Electronics Company, Korea, where he was in charge of the device characterization group. In 1997, he joined the TCAD Group, Intel Corporation, Santa Clara, CA, where he was a Staff Engineer until 2002, where he worked on advanced noise and RF characterization and modeling. In 2002, he joined the System LSI Division, Samsung Electronics Company, Ltd., Gyeonggi-Do, Korea, where he has been leading projects in the area of SiGe HBT, RF CMOS, sub-90-nm advanced device modeling, electrostatic discharge, and input–output designs.

Kang-Wook Park received the B.S. degree in ceramic engineering from Yonsei University, Seoul, Korea, and the M.S. degree in ceramic engineering from Yonsei University, Seoul, Korea, in 1989 and 1995, respectively.

From 1990 to 1995, he was with new process research center of Samsung Electronics Company, Ltd., Gyeonggi-Do, Korea, and worked on high-speed bipolar and BiCMOS process development. In 1996, he moved to the Process Research Center, System LSI Division, Samsung Electronics Company, Ltd. In 2000, he joined the high-speed BiCMOS process development project and production projects. Since 2000, he has taken charge of the high-speed SiGe HBT BiCMOS process development and mass production set up.

Bumman Kim (S'77–M'78–SM'97) received the Ph.D. degree in electrical engineering from Carnegie Mellon University, Pittsburgh, PA, in 1979.

From 1978 to 1981, he was engaged in fiber-optic network component research at GTE Laboratories Inc. In 1981, he joined the Central Research Laboratories, Texas Instruments Incorporated, where he was involved in the development of GaAs power field-effect transistors (FETs) and monolithic microwave integrated circuits (MMICs). He has developed a large-signal model of a power FET, dual-gate FETs for gain control, high-power distributed amplifiers, and various millimeter-wave MMICs. In 1989, he joined Pohang University of Science and Technology, Pohang, Korea, where he is a Professor at the Electronic and Electrical Engineering Department and the Director of the Microwave Application Research Center, and is involved in device and circuit technology for RFICs. In 2001, he was a Visiting Professor of electrical engineering at the California Institute of Technology, Pasadena. He has authored over 200 technical papers. He is a Distinguished Lecturer of the IEEE Microwave Theory and Techniques Society.

Dr. Kim is a member of the Korean Academy of Science and Technology and the Academy of Engineering of Korea. He is the Associate Editor for the IEEE TRANSACTIONS ON MICROWAVE THEORY AND TECHNIQUES.